

DOE/PC/91305-14

DE-FG22-91PC91305-14

**CHARACTERIZATION OF POROSITY VIA SECONDARY  
REACTIONS**

**J.M. Calo (Principal Investigator), Peter J. Hall, M. Mirari  
Antxustegi, and L. Zhang**

**Division of Engineering  
BROWN UNIVERSITY  
Providence, Rhode Island 02912**

**Quarterly Technical Progress Report  
1 January 1995 - 31 March 1995**

**Prepared for:  
U.S. DEPARTMENT OF ENERGY  
Pittsburgh Energy Technology Center  
Pittsburgh, Pennsylvania 15236**

**[ "US/DOE Patent Clearance is not required prior to the publication  
of this document." ]**

**DISTRIBUTION OF THIS DOCUMENT IS UNLIMITED**

*ma*

**MASTER**

## **DISCLAIMER**

This report was prepared as an account of work sponsored by an agency of the United States Government. Neither the United States Government nor any agency thereof, nor any of their employees, make any warranty, express or implied, or assumes any legal liability or responsibility for the accuracy, completeness, or usefulness of any information, apparatus, product, or process disclosed, or represents that its use would not infringe privately owned rights. Reference herein to any specific commercial product, process, or service by trade name, trademark, manufacturer, or otherwise does not necessarily constitute or imply its endorsement, recommendation, or favoring by the United States Government or any agency thereof. The views and opinions of authors expressed herein do not necessarily state or reflect those of the United States Government or any agency thereof.

## **DISCLAIMER**

**Portions of this document may be illegible  
in electronic image products. Images are  
produced from the best available original  
document.**

## SUMMARY

**The following was accomplished during the reporting period:**

- Small angle neutron scattering (SANS) data were obtained for Pittsburgh #8 coal char samples at various levels of burn-off at the Intense Pulsed Neutron Source (IPNS) of the Argonne National Laboratory on the small angle diffractometer (SAD) instrument.
- The Pittsburgh #8 samples complement previous SANS data obtained for non-mineral matter-containing phenol-formaldehyde resin char samples.
- A contrast-matching technique involving the comparison of scattering data for "dry" samples with data from the same samples saturated in deuterated toluene, show that the ungasified Pittsburgh #8 char has very little closed porosity and, consequently, that pore development during gasification proceeds by the creation of new pores. In the early stages of gasification (< 4.5% burn-off) a pore system with significant microporosity is produced. In later stages of gasification (4.5%-13.5% burn-off) the tendency is to open these micropores, producing a pore system with a broad size distribution.
- Nitrogen adsorption isotherms (77K) were determined for all the same samples for which SANS data were obtained in order to provide a corroborative check on their porosity characteristics.

**Plans for the next reporting period:**

Specific plans for the next reporting period include analysis of SANS data obtained for Wyodak and Pocahontas #3 coal char samples. The suite of chars will then encompass coals of varying rank plus the non-mineral matter-containing phenol-formaldehyde resin char.

## 1.0. PROJECT BACKGROUND

### 1.1. *Overview.*

Specific surface area, as well as its accessibility to gaseous reactants, are of paramount importance for all heterogeneous interactions occurring at coal char surfaces. Accessibility of this surface area is governed by the pore structure morphology of the char; i.e., pore size distribution, tortuosity, intersections, shape, etc. The porosity morphology of coal chars varies over a considerable range and is determined by a large number of factors including the nature of the porosity of the precursor material prior to carbonization, the carbonization process, and extent and method of any subsequent activation or gasification. A persistent problem in this area has been the reliable, quantitative measurement and characterization of the resultant porosity, especially the micropores. For example, electron microscopy tends to be qualitative; small angle X-ray or small angle neutron scattering (SAXS/SANS) can suffer from sensitivity to interpretive models, and the inability to distinguish porosity that communicates with the surface from that which does not; and gas adsorption techniques also have several well known drawbacks. The latter, however, are perhaps the most reliable in general, but yield pore size distributions indirectly *via* surface area and pore volume measurements, and can also be laborious and time-consuming. Therefore, there is still a critical need for practical and facile techniques to characterize the porosity of coal chars.

### 1.2. *The Current Project.*

The current project is directed at the development of a new approach to this very old problem. During the course of recent work applying temperature programmed desorption (TPD) to the determination of energetic distributions of oxygen complexes on the surfaces of oxidized coal chars (Calo *et al.*, 1989,

1991), we discovered that secondary interactions occurring within the char structure during TPD produce characteristic features in the resultant spectra that appear to be quite sensitive to char porosity. The relative and absolute extents of these secondary interactions form the basis of a potential characterization technique. The use of such a method to characterize coal char porosity is potentially attractive because the requisite spectra can be obtained in a single TPD experiment -- a very facile experimental procedure. However, the unambiguous and quantitative interpretation of such data in terms of parameters that can be used to characterize coal char porosity still requires development and an improved understanding of the controlling phenomena. These issues define the primary focus of the current work.

The background and general approach of the secondary interaction method for the characterization of porosity was outlined in the first quarterly technical progress report on this grant (DE-FG22-91PC91305-1), and, therefore, it will not be repeated here. Here we report on the progress that has been made in the construction, development and testing of a new TPD-MS/TGA system being developed in our laboratory for the purpose of conducting the temperature programmed desorption experiments for obtaining the secondary interaction data.

The project plan also includes the use of other techniques to characterize porosity in addition to the secondary interaction approach for the purposes of comparison, quantification, and validation. It is noted that at least two other more well established methods will be used in such a manner. Specifically, gas adsorption techniques in our own laboratory, and small angle scattering (SAS) (X-ray (SAXS) and neutron (SANS)). The latter will be accomplished in conjunction with Dr. Peter J. Hall of the Department of Pure and Applied Chemistry of the University of Strathclyde, Glasgow, Scotland. The data will be analyzed using models and computational techniques being developed in our laboratory.

## 2.0. PROJECT WORK

### Porosity Evolution *Via* Contrast-Matching, Small Angle Neutron Scattering (SANS).

#### 2.1. *Background.*

As indicated above, small angle scattering is being used in this project as an auxiliary porosity characterization technique. Although there have been a number of investigations using small angle X-ray scattering (SAXS), the full potential of this technique has not been fully realized due to a number of factors including problems such as the role of "closed" porosity. Recently, however, we have made progress in the understanding of the issue of "closed" and "open" porosity by using contrast-matching, small angle neutron scattering (SANS) (DE-FG22-91PC91305-10).

In a previous set of experiments conducted at the Intense Pulsed Neutron Source (IPNS) of the Argonne National Laboratory, we obtained data on phenol-formaldehyde resin char samples. This material is intended to be representative of a non-mineral matter-containing char. As with SAXS, in SANS scattering off the char samples is due to "open" and "closed" porosity, as well as interparticle scattering. However, when the samples are saturated with deuterated toluene, the solvent fills all accessible porosity and interparticle voids. Since deuterated toluene has about the same neutron scattering density as typical polycrystalline carbon ( $\sim 5.6 \text{ } 10^{10} \text{ cm}^{-2}$ ), it contrast-matches the carbon very closely. Thus, with respect to neutrons, there is no scattering contrast between the carbon and deuterated toluene in the pores and no coherent scattering. In other words, the "open" porosity becomes "invisible" to the neutrons, and neutron scattering from the deuterated toluene/char mixture is due to carbon and any porosity that could not be accessed by the deuterated toluene. It was shown that there was significant residual scattering in the contrast-matched samples which was due to a well developed closed pore system. The difference between the dry and contrast-

matched samples is, therefore, due to scattering from the open pores and interparticle scattering from the external surfaces of the particles. Nitrogen adsorption at 77K showed that the ungasified resin char had a low surface area (< 2m<sup>2</sup>/g) and thus very low levels of open microporosity. "Difference" scattering in this case was dominated by interparticle scattering. It was then demonstrated that pore development in the resin char upon activation was primarily due to the opening of "closed" porosity.

More recently, we have collected additional data on three chars derived from coals obtained from the Argonne Premium Coal Sample Bank (Vorres, 1993): Pittsburgh #8, (high volatile bituminous), Pocahontas #3 (low volatile bituminous), and Wyodak (subbituminous). In the current report we present an analysis of the Pittsburgh #8 data and compare the results with those obtained for the resin char.

## ***2.2. Experimental.***

As indicated above, analysis of porosity *via* contrast-matching involves the comparison of SANS data from two experiments on: (1) the dry, powdered sample; and (2) the same sample saturated with deuterated toluene. In the latter case, toluene fills all accessible porosity and interparticle voids. The difference between the dry and contrast-matched samples is then due to scattering in "open" pores, and interparticle scattering.

SANS data were obtained with the small angle diffractometer at the Intense Pulsed Neutron Source of the Argonne National Laboratory. Suprasil sample holders with a 2 mm path length were used. The data were corrected for scattering from the sample holder and for other instrumental backgrounds. Normalization for the sample thickness and transmission were made and the data were scaled to yield absolute calibrations.

Pittsburgh #8 is a coking coal which upon slow pyrolysis yields a very low surface area char with little microporosity, unlike phenolic resin char (DE-

FG22-91PC91305-10). Coal samples were heated under nitrogen at 10 K/min to 1273K with a soak time of 1h. The resultant char was ground to between 60 and 100 Tyler mesh. For contrast-matching, samples were mixed with excess deuterated toluene and placed in an ultrasonic bath for 4h. Activation of the char was performed in air in a tube furnace at 673K

### 2.3. Results and Discussion.

Figure 1a presents the nitrogen adsorption isotherms for the coal char samples. For clarity, the isotherm for the ungasified char is shown on an expanded scale in Figure 1b. The nitrogen surface area of the ungasified char was  $8 \text{ m}^2/\text{g}$ , which suggests no significant open porosity, which is typical of chars from coking coals. The isotherm is of Type II according to the BDDT (1940) classification, which is typical for nonporous materials or materials which have pore systems with significant amounts of meso- or macroporosity.

The SANS data for the unactivated char are presented in Figure 2a,b. The “dry” curve shows no significant scattering for  $q > 0.15 \text{ \AA}^{-1}$ , which suggests the absence of scatterers of less than  $\sim 40 \text{ \AA}$ , and the absence of well developed microporosity, consistent with the  $\text{N}_2$  adsorption data. The monotonic increase in scattering with decreasing  $q$  indicates that the size of the largest scatterer cannot be resolved. This may be due to either interparticle scattering or scattering from a small number of large pores.

Guinier (1955) found that the small angle scattering intensity of scattering vector values approaching zero (i.e.,  $q \rightarrow 0$ ) is well approximated by:

$$I(q) = I(0) \exp(-q^2 R_g^2/3) \quad [1]$$

where  $I(0)$  is the scattering intensity at zero scattering vector (i.e.,  $q = 0$ ), and the scattering radius of gyration,  $R_g$ , is a measure of the size of scatterers, analogous to the radius of gyration as defined for classical mechanics. Hence,  $R_g$ , is a measure of the size of the scattering porosity, for example. Taking the logarithm of both sides of Eq. [1] yields:

$$\ln\{I(q)\} = \ln\{I(0)\} - q^2 R_g^2/3 \quad [2]$$

Thus, a plot of  $\ln\{I(q)\}$  vs.  $q^2$ , which is known as a Guinier plot, should be a straight line with a slope of  $-R_g^2/3$ . Linear behavior of this type is interpreted as being indicative of scatterers of a single, predominant size. However, the Guinier plot of the data in Figure 2, presented in Figure 3, exhibits curvature over the entire  $q$  range, which is suggestive of a broad range of pore sizes.

From Figure 2 it can be seen that contrast-matching significantly reduces the scattered intensity at all  $q$ -values. In order to emphasize this point, the scattering data are presented on a linear scale in Figure 2b. The integral under the "dry" data is 2.19 and that under the contrast-matched curve is 0.10 (arbitrary units). Thus, scattering has been reduced by a factor of 22, and about 4.8% of the total scattering is due to closed porosity. This is compared to 59.9% for the unactivated phenolic resin char (Hall *et al.*, 1994). Figure 2 also shows that there is no significant scattering for  $q > 0.078 \text{ \AA}^{-1}$  for the contrast-matched sample, which suggests the absence of porosity less than  $\sim 75\text{\AA}$ . It is most probable, therefore, that scattering is due to a small number of large pores. The result is that the dry and difference curves in Figure 2 are very similar.

Activation to 0.8% burn-off increases the  $N_2$  surface area to  $80 \text{ m}^2/\text{g}$ , consistent with porosity development. Figure 1 shows a BDDT Type II adsorption isotherm for this char sample, although the knee is more clearly defined than for the ungasified (0% burn-off) char. This suggests the development of significant levels of microporosity. The SANS data for the 0.8% burn-off char are shown in Figure 4. The results are qualitatively the same as for the ungasified char. The integral for the dry sample scattering data is 3.33, which decreases to 0.15 (arbitrary units) for the contrast-matched sample. Therefore, 4.8% of the total scattering is due to closed porosity, which is the same as for the ungasified (0% burn-off sample).

A comparison of the scattering from the contrast-matched samples in Figures 2 and 4, presented in Figure 5, shows that they are very similar. This

constitutes evidence that the scattering is indeed from closed porosity which is unaffected by gasification. The scattering data from the 0% and 0.8% samples indicate that gasification proceeds by the creation of new porosity, rather than the opening of closed porosity as is the case for phenolic resin char.

The "dry" scattering curve in Figure 4 is typical for a material with a well developed micropore system. For convenience, the scattering behavior for Porod (1952) type of behavior (i.e.,  $I \propto h^{-3}$ ) is also shown in Figure 4. The upward deviation from the Porod curve is due to the presence of micropores formed during gasification.

Since the ungasified char has a low surface area, and the adsorption isotherm for this char is typical for a non-porous material, the scattering in the "difference" curve of Figure 2 is, therefore, dominated by interparticle effects; i.e., scattering determined by the external surface of the char particles. This effect was also observed for the resin char. The form of the scattering curve for the ungasified sample closely approximates Porod behavior, which suggests that it is due to the presence of relatively large-scale scatterers.

Since the surface area of the 0.8% gasified char suggests the development of open porosity, then the difference curve in Figure 4 must contain information about interparticle scattering as well as the additional porosity. The "difference" curves for the 0% and 0.8% burn-off char samples are compared in Figure 6. The curves converge at low  $q$  values, which suggests that the nature of the background scattering is not significantly different in the two cases. The difference between the two "difference" curves (i.e.,  $(0.8\%_{\text{diff}} - 0\%_{\text{diff}})$  in Figure 6) is, therefore, due to scattering from any additional porosity created during gasification. In this manner, the 0% burn-off "difference" curve can be used to correct the "difference" curves at other burn-offs for interparticle scattering effects.

Figure 1 shows that the  $N_2$  BET surface areas increase with burn-off. The surface area at 13.5% burn-off is  $252 \text{ m}^2/\text{g}$ . The isotherms are all of Type II,

although the "knee" seems to be more clearly defined for the 0.8% and 4.5% gasified chars. The corresponding SANS data for all the Pittsburgh #8 samples are presented in Figure 7. These are "difference" scattering curves that have been corrected for interparticle scattering, as discussed above, using the 0% burn-off data presented in Figure 2. These curves provide information about pores that develop during gasification. The Guinier analyses for these data sets are presented in Figure 8. As discussed above, scattering for the 0.8% gasified char is typical of a pore network that contains a significant amount of microporosity. Guinier analysis shows a linear portion of the data with a radius of gyration,  $R_g=16.3\text{\AA}$ . Therefore, the early stages of gasification appear to produce microporosity. The scattering curve for the 4.5% gasified char in Figure 7 is also typical of a microporous network, and the corresponding Guinier plot in Figure 8 is also linear with  $R_g=13.5\text{\AA}$ . This indicates that further microporosity has been produced. In contrast, the scattering curve for the 13.5% gasified char is typical of a pore system with a wide range of pore sizes. The corresponding Guinier plot in Figure 8 confirms this by showing curvature over the entire range of  $q$  values. The log-log plot is linear over the range  $0.0058\text{\AA}^{-1} < q < 0.054\text{\AA}^{-1}$  and the slope of the line is -3.8. This deviates slightly from ideal Porod behavior and is probably due to fractal roughening of the pore surfaces. The fractal dimension is 2.2, which agrees with other fractal investigations of gasified carbon surfaces. Therefore in the range 4.5%-13.5% burn-off micropores appear to be opened to produce a pore system with a wide size range.

#### **2.4. Conclusions.**

As with our previous work with resin char, contrast-matching has been shown to be a very useful technique for investigating the development of porosity in carbons both in terms of understanding the effects of closed porosity and the elimination of interparticle scattering. Contrast-matching SANS shows that Pittsburgh #8 char has very little closed porosity and, consequently, that pore

development during gasification proceeds by the creation of new pores. In the early stages of gasification (<4.5% burn-off) a pore system with significant microporosity is produced. In later stages of gasification (4.5%-13.5% burn-off) the tendency is to open these micropores, producing a pore system with a broad size distribution.

### **3.0. PLANS FOR NEXT REPORTING PERIOD**

Work will continue along the two-pronged mode of attack involving thermal desorptions of oxidized samples in the TPD-MS/TGA system, and porosity characterization using gas adsorption techniques and the analysis of small angle scattering data. Specific plans for the next reporting period include analysis of SANS data obtained for Wyodak and Pocahontas #3 coal char samples. The suite of chars will then encompass coals of varying rank plus the non-mineral matter-containing phenol-formaldehyde resin char.

### **REFERENCES**

Brunauer, S., Deming, L.S., Deming, W.S. and Teller, E., *JACS* **62**, 1723 (1940).

Guinier, A. and Fournet, G., in *Small Angle Neutron Scattering*, translated by C.B. Walker, K.L. Kudowitch, Wiley, N.Y., 1955, pp. 19-23.

Hall P.J., Antxustegi, M.M. and Calo, J.M. *Proc. Carbon '94*, Granada, Spain, 1994, p.164.

Porod, G., *Kolloid Zeitschrift* **124**, 83 (1951); **125**, 108 (1952).

Vorres, K.S., *Users Handbook for the Argonne Premium Coal Samples*, ANL/PCSP-93/1, U.S.D.O.E., Argonne, IL, 1993.

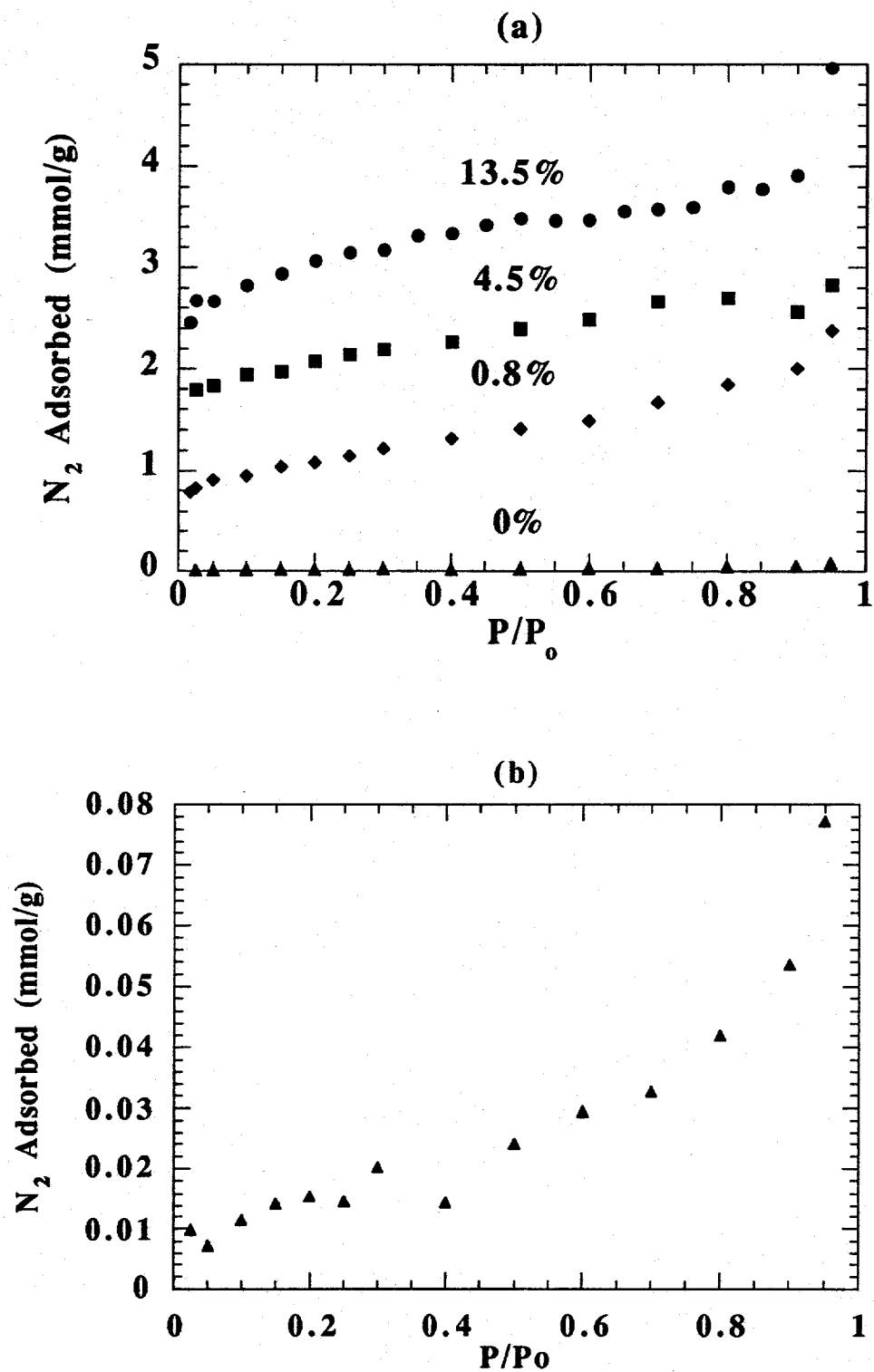


Figure 1.(a) Nitrogen adsorption isotherms for Pittsburgh #8 coal char samples at various burn-offs. (b) 0% burn-off on expanded scale.

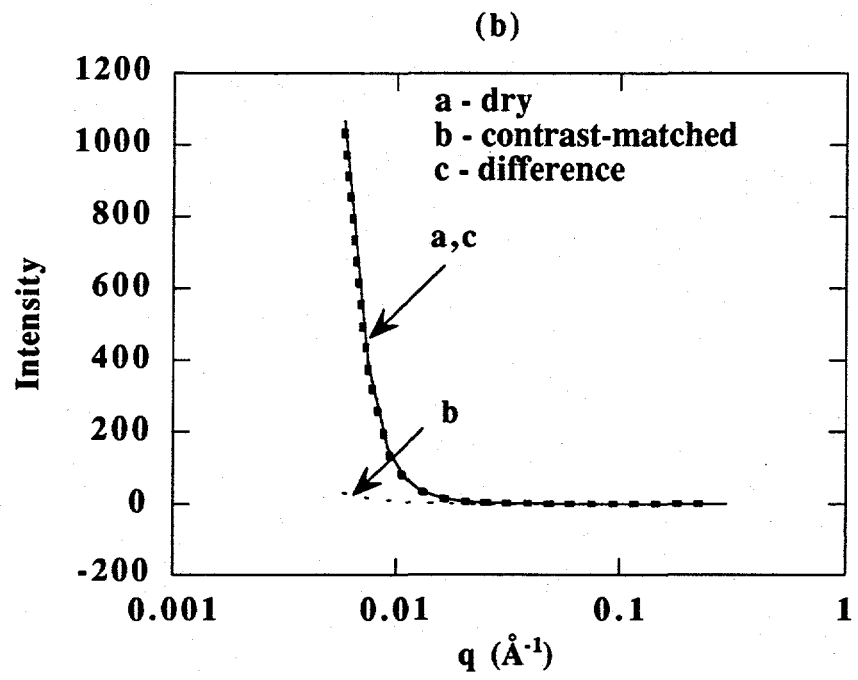
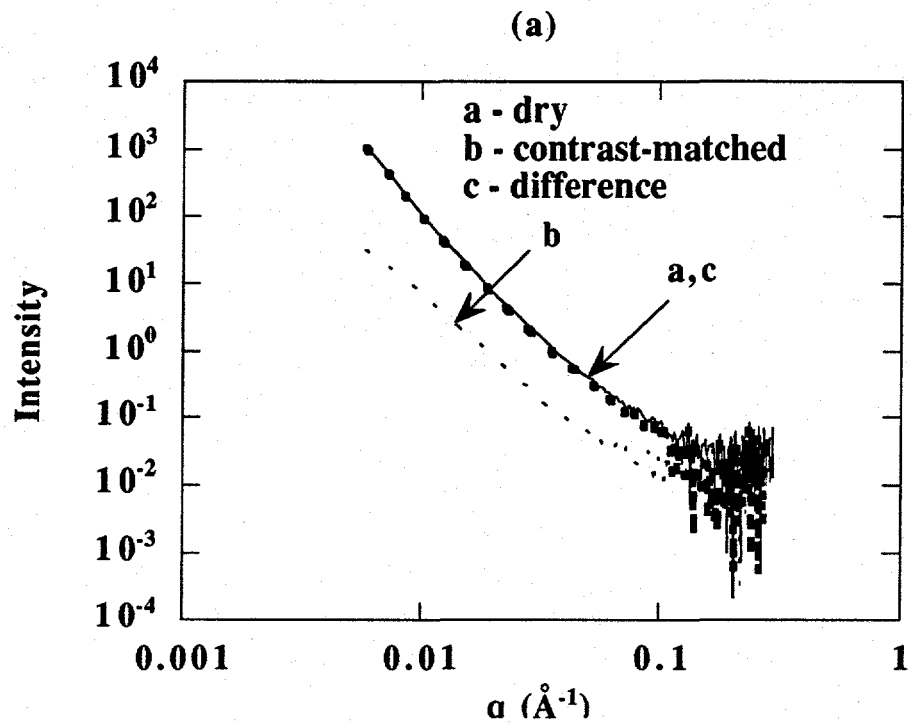


Figure 2. (a) Scattering data for ungasified (0% burn-off) Pittsburgh #8 coal char sample. (b) linear scale for scattering intensity.

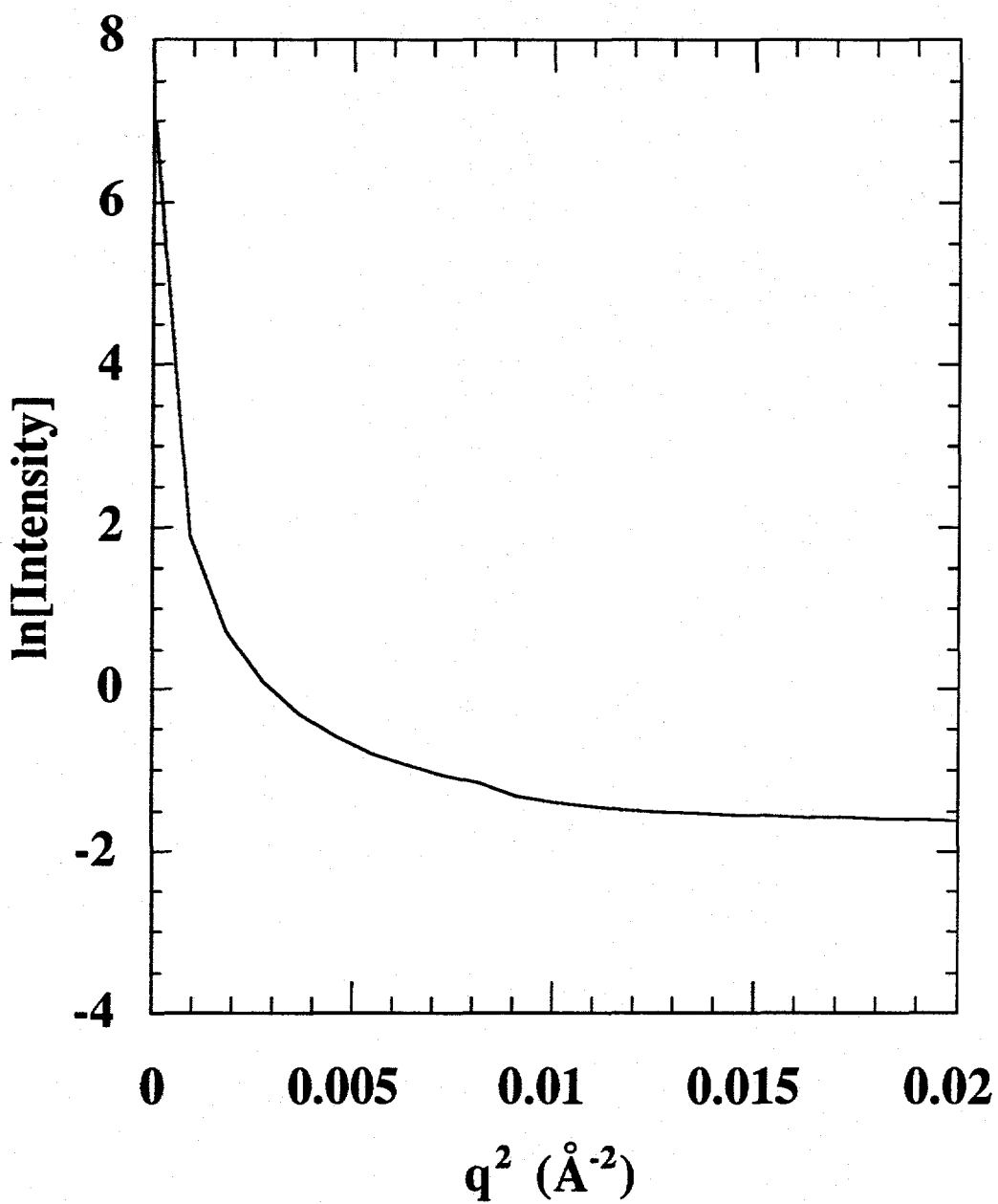


Figure 3. Guinier plot of scattering data for ungasified (0% burn-off) Pittsburgh #8 coal char sample.

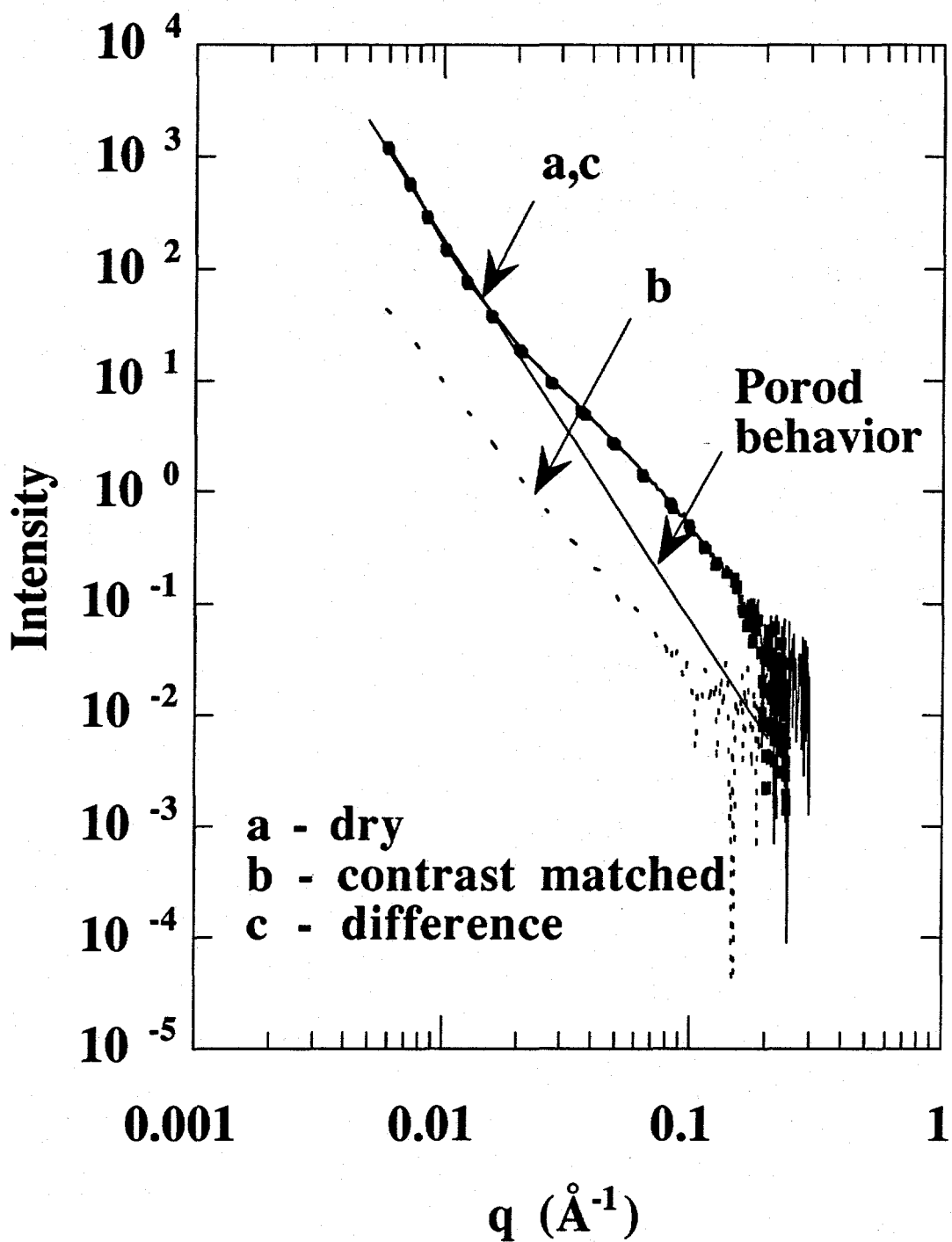


Figure 4. Small angle neutron scattering from Pittsburgh #8 coal char gasified to 0.8% weight loss in air at 673K: (a) dry; (b) contrast-matched by mixing with deuterated toluene; and (c) difference between scattering curves (a) and (b).

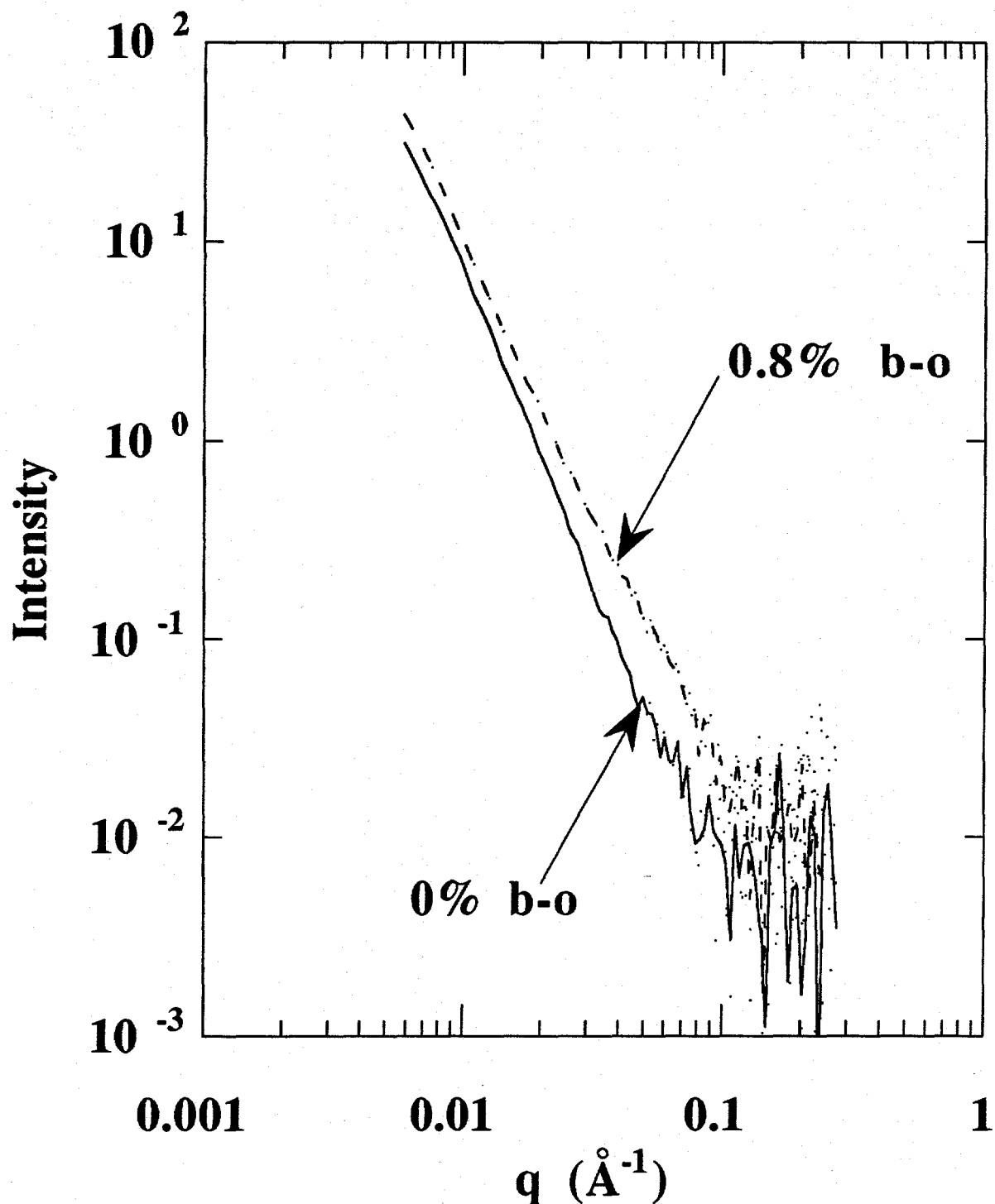


Figure 5. Contrast-matched scattering curves for 0% and 0.8% burn-off Pittsburgh #8 coal char samples.

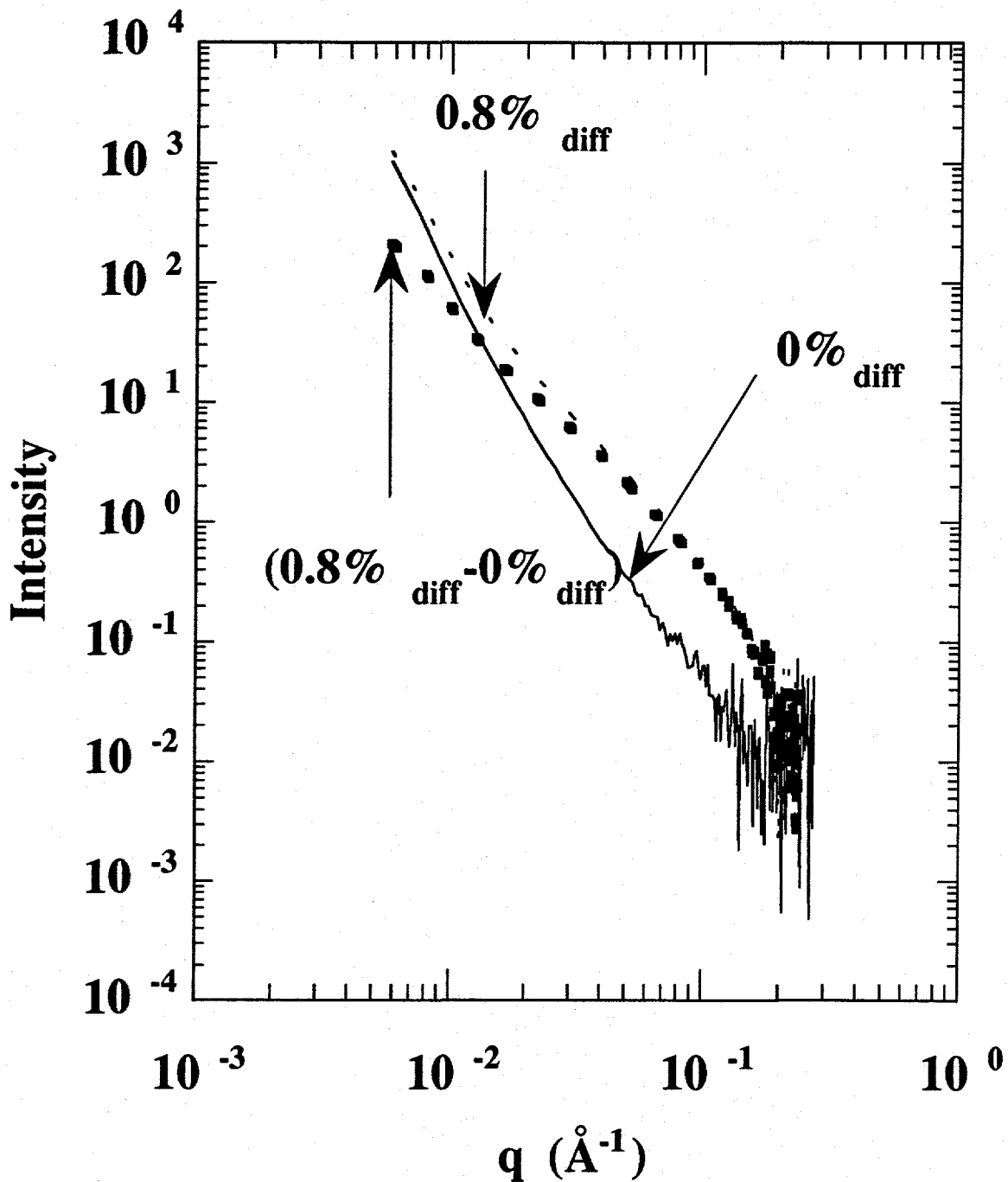


Figure 6. Method for correcting the "difference" scattering curve (curve (c) in Figure 4) by subtraction of the interparticle scattering (curve (c) in Figure 2) to show scattering from pores produced during gasification (0.8%<sub>diff</sub>-0%<sub>diff</sub>) for Pittsburgh #8 coal char gasified to 0.8% burn-

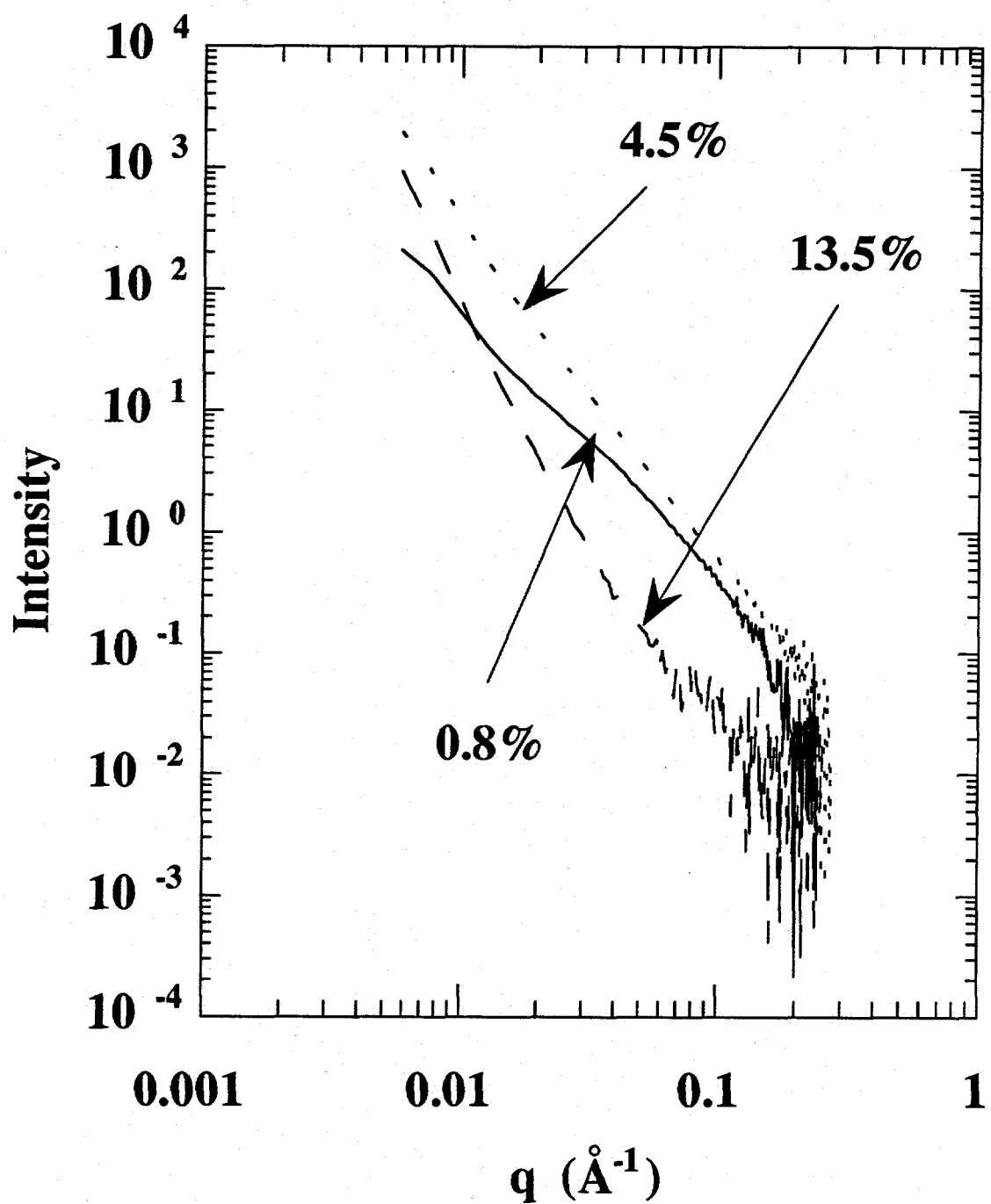


Figure 7. Scattering data for Pittsburgh #8 samples as a function of burn-off.

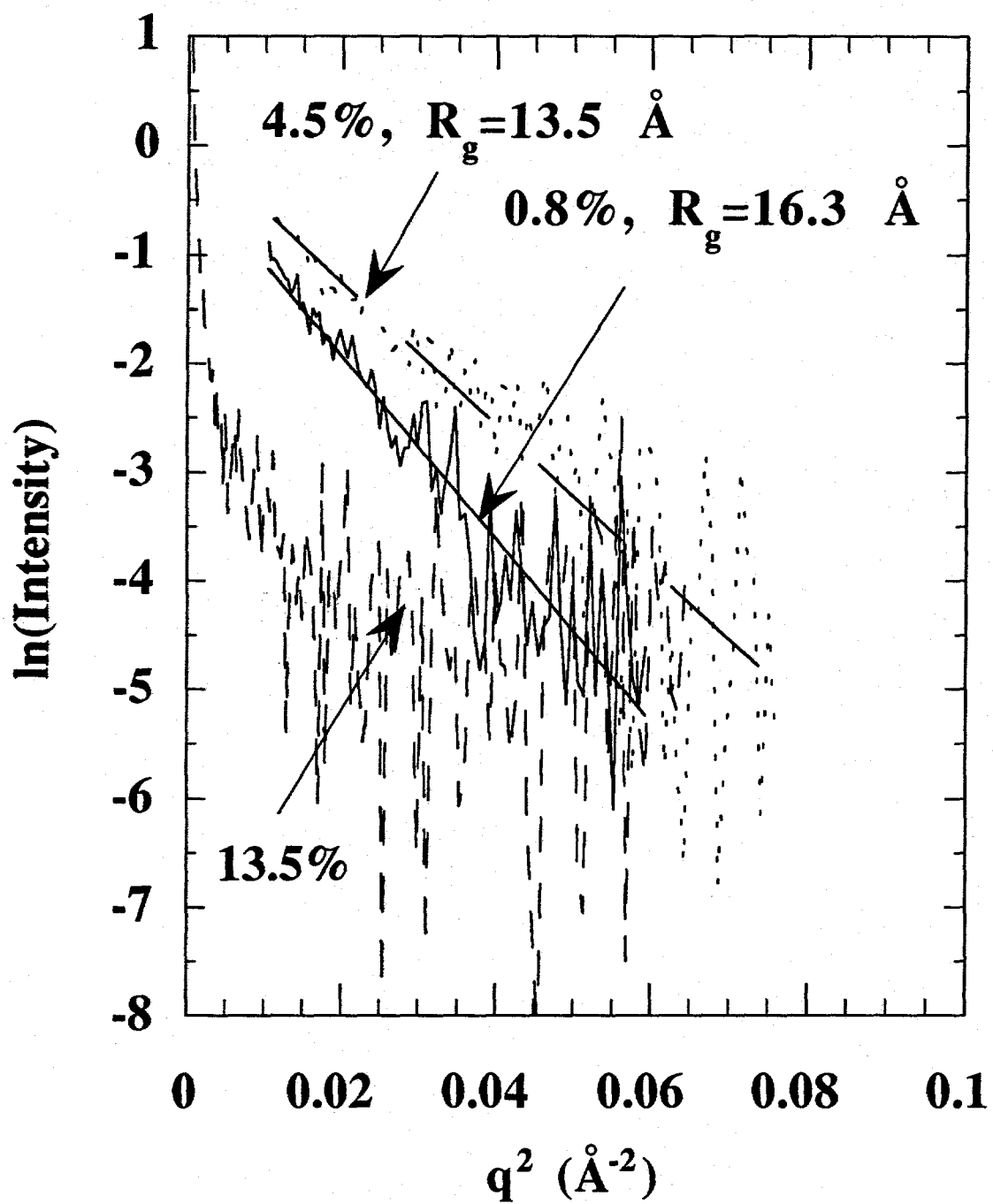


Figure 8. Guinier plots of scattering data from Figure 7 for Pittsburgh #8 samples as a function of burn-off.